



ELSEVIER

Journal of Computational and Applied Mathematics 72 (1996) 379–392

---

JOURNAL OF  
COMPUTATIONAL AND  
APPLIED MATHEMATICS

---

# Numerical stability analysis and computation of Hopf bifurcation points for delay differential equations

Tatyana Luzyanina<sup>a</sup>, Dirk Roose<sup>b,\*</sup>

<sup>a</sup>*Institute of Mathematical Problems in Biology, RAS, Pushchino, Moscow region, 142292, Russia*

<sup>b</sup>*Department of Computer Science, Katholieke Universiteit Leuven, Celestijnenlaan 200A, B-3001 Heverlee-Leuven, Belgium*

Received 28 September 1995

---

## Abstract

We present a numerical technique for the stability analysis and the computation of branches of Hopf bifurcation points in nonlinear systems of delay differential equations with several constant delays. The stability analysis of a steady-state solution is done by a numerical implementation of the argument principle, which allows to compute the number of eigenvalues with positive real part of the characteristic matrix. The technique is also used to detect bifurcations of higher singularity (Hopf and fold bifurcations) during the continuation of a branch of Hopf points. This allows to trace new branches of Hopf points and fold points.

**Keywords:** Delay differential equations; Numerical stability analysis; Hopf bifurcation; Continuation

**AMS classification:** 65J15, 65P05

---

## 1. Introduction

The development of the theory of delay differential equations (DDEs) was initiated by taking into account the fact that the behaviour of physical systems not only depends on their present state, but also on their past history. DDEs have many applications in the theory of control systems, the theory of self-oscillating systems, in biological, chemical and physical problems with a feedback mechanism, and in many other areas of science and engineering, the number of which is steadily expanding.

The general theory and basic results for DDEs have been comprehensively presented in the well-known books of Hale [13], Bellman and Cooke [3], El'sgol'ts and Norkin [9], Driver [8], Kolmanovskii and Myshkis [19] and subsequent articles by many authors. Research on numerical

---

\* Corresponding author. e-mail: dirk.roose@cs.kuleuven.ac.be.

techniques for DDEs has focused until now on time integration. There is an extensive literature on numerical methods for solving DDEs and the numerical stability of these methods (a bibliography is given in [1]). Some numerical methods have been developed to approximate a DDE system by a system of ODEs of high dimensionality. This finite-dimensional approach is usually applied to test the stability properties of an attractor of the DDE system (see, for example, [2, 10, 4]). The drawback of this approach is that a very accurate approximation is necessary in order to check stability, which leads to a very expensive method.

The existence of periodic solutions in DDEs is a topic of interest in many applications. Periodic solutions can arise via Hopf bifurcation, i.e., when a steady-state solution loses its stability as a physical parameter crosses a critical value. Although the theory of Hopf bifurcation in DDEs is now well understood (see, for example, [14–16]), its practical application still poses many significant computational problems. The detection and computation of Hopf bifurcation points, the direction of the bifurcating branches, as well as the amplitude, period and stability of periodic solutions in DDEs are major tasks in applications. Many techniques have been developed to treat such problems (for example, the method of averaging [5, 6], the use of the Poincaré normal form [16], the method of Liapunov–Schmidt [7, 22, 11]). Each of these methods is well suited for bifurcation analysis in specific applications but cannot be applied to a general nonlinear system of equations with several delays. Moreover, while there are well-developed numerical techniques and software packages for bifurcation analysis of ordinary differential equations (ODEs) (see, e.g., [21, 18] for references), numerical methods and software, which are suited for general systems of DDEs, are largely lacking.

In this paper we present a numerical technique for the stability analysis and the computation of branches of Hopf bifurcation points in nonlinear systems of DDEs with several constant delays. The detection and computation of Hopf bifurcation points is important for the bifurcation analysis of periodic solutions in systems of DDEs as well as in ODE systems. Note that computation of branches of steady-state solutions of DDE systems can be realized via continuation methods for the ODE case. Indeed, a system of DDEs and the system of ODEs, obtained from the former by setting all delays to zero, have the same steady-state solutions. So, we consider the computation of Hopf bifurcation points as the first step in the numerical bifurcation analysis of DDEs. The presented technique works within the framework of the LOCBIF software package [18], which was created for the analysis of local bifurcations of (a) equilibrium points and periodic solutions of ODEs, and (b) fixed points and periodic orbits of iterated maps. This package can be extended to allow the bifurcation analysis of DDEs.

Section 2 is devoted to the stability analysis of a steady-state solution of a system of DDEs. We present a numerical implementation of the argument principle to compute the number of roots with positive real part for a characteristic equation of general type arising in the stability analysis of DDEs. Its application to the stability analysis of Hopf bifurcation points is discussed. In Section 3 we introduce a nonlinear algebraic system, that can be used as a determining system for Hopf bifurcation points. A continuation procedure applied to this determining system allows to trace branches of Hopf points and to detect bifurcations of higher singularity during the continuation of these branches. This allows to trace new branches of Hopf points and fold points. Results of the application of the considered technique to a system of DDEs, derived from the Olmstead model for viscoelastic flow, are presented in Section 4. In Section 5 we summarize the main results.

## 2. Stability analysis using the argument principle

We consider the following system of DDEs:

$$\frac{dx}{dt} = F(x(t), x(t - \tau_1), \dots, x(t - \tau_m), \mu), \quad (1)$$

where  $x(t)$  is an  $n$ -dimensional vector of phase variables;  $\tau_i$ ,  $i = 1, \dots, m$ , are the time delays ( $\tau_i > 0$ );  $\mu$  is a  $k$ -dimensional vector of parameters;  $F$  is a nonlinear  $n$ -dimensional vector-valued function,  $F: \Omega \times C \rightarrow \mathbb{R}^n$ ,  $\Omega$  is the parameter space,  $\Omega \subset \mathbb{R}^k$ ,  $C = C([-r, 0], \mathbb{R}^n)$  is the Banach space of continuous functions mapping the interval  $[-r, 0]$  into  $\mathbb{R}^n$ ,  $r = \max_i \tau_i$ ,  $\mathbb{R}^n$  is an  $n$ -dimensional linear vector space.

The characteristic matrix of (1) is

$$\Delta(x^0, \mu^0, \lambda) = \lambda I - \sum_{i=0}^m A_i(x^0, \mu^0) e^{-\tau_i \lambda}, \quad (2)$$

where  $x^0$  is a steady-state solution of (1) for  $\mu = \mu^0$ ,  $\lambda$  is an eigenvalue,  $I$  is the  $n \times n$  identity matrix,  $\tau_0 = 0$ ,  $A_i$ ,  $i = 0, 1, \dots, m$ , are  $n \times n$  constant matrices such that

$$F(x(t), x(t - \tau_1), \dots, x(t - \tau_m), \mu) = \sum_{i=0}^m A_i(x^0, \mu^0) x(t - \tau_i) + f(x(t), x(t - \tau_1), \dots, x(t - \tau_m), \mu),$$

where  $f$  contains the nonlinear terms. The characteristic equation  $\det \Delta(x^0, \mu^0, \lambda) = 0$  can be written as

$$P(\lambda) = \sum_{i=0}^m p_i(\lambda) e^{-\tau_i \lambda} = 0, \quad (3)$$

where each  $p_i(\lambda)$  is a polynomial in  $\lambda$  of degree at most  $n$ :

$$p_i(\lambda) = p_{i0} + p_{i1} \lambda + \dots + p_{im_i} \lambda^{m_i} \quad (m_i \leq n).$$

The problem of analysing the location, in the complex plane, of the zeros of a general polynomial  $P(\lambda)$  of the form (3) is a nontrivial problem. This is especially true when the dimension  $n$  of the system and/or the number of delays  $m$  is large. Below we show how the stability analysis of a steady-state solution of (1) can be done numerically.

To test the stability of a regular steady-state solution, we do not need to know the actual location of the zeros  $\lambda = \alpha + i\omega$  of (3), but only whether all zeros have negative real part ( $\alpha < 0$ ). During the computation of branches of Hopf bifurcation points ( $\lambda^H = i\omega^H$ ) of (1), we are interested in the stability properties of Hopf points, as well as in the variation in the number of eigenvalues with positive real part along a branch of Hopf points in order to detect bifurcations during the continuation of this branch. For this reason, the stability analysis of steady-state solutions of (1) can be done by means of a test on the sign of the real parts of all roots of (3). Several such tests, most often used for certain applications in the context of the stability analysis of steady-state solutions of DDEs, are given in [3, 9]. Among such tests, the argument principle (discussed in detail in [3], its modification for a specific form of (3) is considered in [9]) is most suited for the numerical

implementation and for the application to a general exponential polynomial (3). In practice, the argument principle is often used to compute the number of zeros of an analytic function  $g(z)$  in a bounded domain, as the first step to compute all zeros of  $g(z)$  (see e.g. [24] for references). The authors of [24] have developed a reliable argument principle algorithm to treat this problem. This algorithm uses global information in the form of an upper bound  $M$  for  $|g''(z)|$  over line segments of the boundary of the considered domain. In [25] it is shown that such information is necessary to assure that the algorithm is reliable, and an automatic way of computing  $M$  is suggested. The developed procedure can only be applied to explicitly given functions  $g(z)$ , while in some applications the explicit expression of  $g(z)$  may not be available. Our numerical implementation of the argument principle is simple and well suited to be used in a continuation procedure (note that we wish to test the stability of each Hopf point along a branch). Furthermore, it does not require the explicit expression of the characteristic equation (3) which can be very complicated for a large system of DDEs with several different delays. The reliability of the results obtained can be checked numerically.

The argument principle is based on the theorem on the logarithmic residue [9], and it is convenient to state this theorem below.

**Theorem** (El'sgol'ts and Norkin [9]). *Suppose that  $G(z)$  is an analytic function except for poles inside and on a closed contour  $C$ , that  $G(z)$  is not zero on  $C$  and has only a finite number of polar singularities within the contour. Then*

$$\frac{1}{2\pi i} \int_C \frac{G'(z)}{G(z)} dz = N_C - Q_C,$$

where  $N_C$  is the number of zeros and  $Q_C$  is the number of poles of  $G(z)$  in the interior of  $C$ , counted according to their multiplicities.

The geometric interpretation of this theorem leads to the argument principle

$$\frac{1}{2\pi} \Delta_C \arg G(z) = N_C - Q_C, \quad (4)$$

where  $\Delta_C \arg G(z)$  is the total increase of the argument of the function  $G(z)$  as  $z$  moves once around the contour  $C$  in the positive direction.

There is also the following restatement of the argument principle. The mapping  $Z = G(z)$  carries each point  $z$  into a corresponding point  $Z$  and, hence, a closed contour  $C$  in the  $z$ -plane into a closed contour  $J$  in the  $Z$ -plane. Then the difference  $N_C - Q_C$  is equal to the number of times the curve  $J$  under the mapping  $Z = G(z)$  encircles the origin in the  $Z$ -plane.

We use the formulation (4) since it is more suited for numerical computation. Consider a closed contour  $C$  lying to the right of the imaginary axis such that polynomial (3) is not zero on  $C$ . Then, since (3) is an analytic function, the argument principle can be applied, and in accordance with it the number of zeros of  $P(\lambda)$  within  $C$  is equal to  $1/2\pi$  times the variation of the argument of  $P(\lambda)$  as  $\lambda$  moves once around  $C$  in the counterclockwise sense (a zero of multiplicity  $k$  is counted  $k$  times). Note that in our case  $Q_C = 0$ .

The argument of  $P(\lambda)$  is a multivalued function of  $\lambda$ , and its value may vary by  $\pi k$  ( $k \neq 0$ ) as  $\lambda$  varies continuously around  $C$ . So, starting from a point  $\lambda_s$  on  $C$ , we compute the number of times the argument of  $P(\lambda)$  crosses the value  $\pi/2$  or  $-\pi/2$ , increasing or decreasing, when  $\lambda$  varies around the contour  $C$ . Fig. 1 illustrates the variation of  $\arg P(\lambda) \pmod{\pi/2}$  for an unstable steady-state solution of the system of DDEs considered in Section 4 (here  $N$  denotes the numbering of the points on the contour). We can see that the total increase of  $\arg P(\lambda)$  along a considered contour is equal to  $2\pi$ . This means that there is one eigenvalue with positive real part within this contour. In applying the argument principle, it is important that  $\arg P(\lambda)$  varies continuously with  $\lambda$ , and that the variation of  $\arg P(\lambda)$  is independent of the particular value of  $\arg P(\lambda_s)$  with which we start. Note that to use the argument principle we do not need to know the explicit expression of polynomial (3). It is sufficient to compute  $P(\lambda)$  numerically as the value of  $\det \Delta(x^0, \mu^0, \lambda)$  at each point  $\lambda = \alpha + i\omega$  along the contour  $C$ .

To determine the stability of a regular steady state, i.e., to compute the number of eigenvalues with positive real part, it is possible to apply the argument principle to a rectangular contour with vertices  $(0, -i\omega_{\max})$ ,  $(\alpha_{\max}, -i\omega_{\max})$ ,  $(\alpha_{\max}, i\omega_{\max})$ ,  $(0, i\omega_{\max})$ , where  $\alpha_{\max} > 0$ ,  $\omega_{\max} > 0$ . Because of the finite size of this contour the method does not guarantee the correct result. Nevertheless, practical application of the method gives good results if large values of  $\alpha_{\max}$  and  $\omega_{\max}$  are used. Anyway, to be sure that the result is correct, it is sufficient to increase values of  $\alpha_{\max}$  and  $\omega_{\max}$  and repeat the procedure.

Stability analysis of bifurcation points on steady states branches is a special case. Since for Hopf points,  $P(\lambda)$  is equal to zero on the imaginary axis, this axis cannot be used as a part of the contour

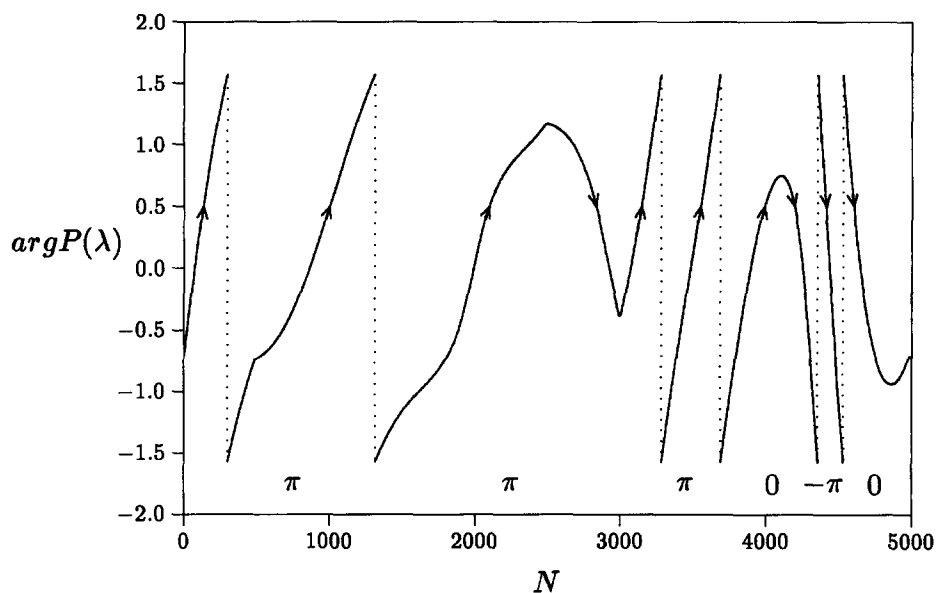


Fig. 1. The variation of the  $\arg P(\lambda) \pmod{\pi/2}$  along a contour for an unstable steady-state solution of the system (10).  $N$  denotes the numbering of the points along the contour. Values  $\pm\pi$  and 0 mean the variation of the  $\arg P(\lambda)$  on the corresponding part of the contour.

$C$ , but we can compute the number of zeros of  $P(\lambda)$  within the rectangle with vertices  $(\alpha_{\min}, -i\omega_{\max})$ ,  $(\alpha_{\max}, -i\omega_{\max})$ ,  $(\alpha_{\max}, i\omega_{\max})$ ,  $(\alpha_{\min}, i\omega_{\max})$ , where  $\alpha_{\max} > \alpha_{\min} > 0$ ,  $\omega_{\max} > 0$ . In this case, the points  $\lambda = \alpha_{\min} \pm i\omega^H$  lying on this contour can be close to eigenvalues  $\lambda^H = \pm i\omega^H$ . We now show that the choice of the step size  $h$  along the contour  $C$  is important, especially when a zero of  $P(\lambda)$  is close to  $C$ . Writing

$$P(\lambda) = P_{\text{Re}}(\lambda) + iP_{\text{Im}}(\lambda), \quad \arg P(\lambda) = \tan^{-1} \frac{P_{\text{Im}}(\lambda)}{P_{\text{Re}}(\lambda)},$$

$$\frac{d(\arg P(\lambda))}{d\lambda} = \frac{1}{P_{\text{Re}}^2 + P_{\text{Im}}^2} \left( P_{\text{Re}} \frac{dP_{\text{Im}}}{d\lambda} - P_{\text{Im}} \frac{dP_{\text{Re}}}{d\lambda} \right),$$

we see that  $d(\arg P(\lambda))/d\lambda \rightarrow \infty$  if  $\lambda \rightarrow \lambda_0$  where  $\lambda_0$  is a zero of  $P(\lambda)$  ( $P_{\text{Re}}(\lambda_0) = 0$ ,  $P_{\text{Im}}(\lambda_0) = 0$ ). This implies that if a point  $\lambda_c$  lying on  $C$  is close to a zero of  $P(\lambda)$ , the value  $d(\arg P(\lambda))/d\lambda$  in the neighbourhood of  $\lambda_c$  can be very large. In this case, if the value of  $h$  is not small enough, we can obtain a wrong value of the variation of  $\arg P(\lambda)$ , by missing values  $\pi k$  and/or  $-\pi k$  ( $k \neq 0$ ).

We have computed numerically the variation of  $\arg P(\lambda)$  for a Hopf point of the system of DDEs considered in Section 4, for which the characteristic matrix has a pair of purely imaginary eigenvalues  $\lambda^H \simeq \pm 0.9832i$ . The results are shown in Fig. 2 for different values of the step size  $h$  (here  $N$  denotes the numbering of the points on the contour for  $h = 10^{-4}$ ). We check the number of zeros of  $P(\lambda)$  within the rectangular contour with vertices  $(10^{-3}, -i)$ ,  $(5 \cdot 10^{-2}, -i)$ ,  $(5 \cdot 10^{-2}, i)$ ,  $(10^{-3}, i)$ , starting from the point  $\lambda = 10^{-3} - i$  and moving along the rectangle with  $h = 5 \cdot 10^{-3}$

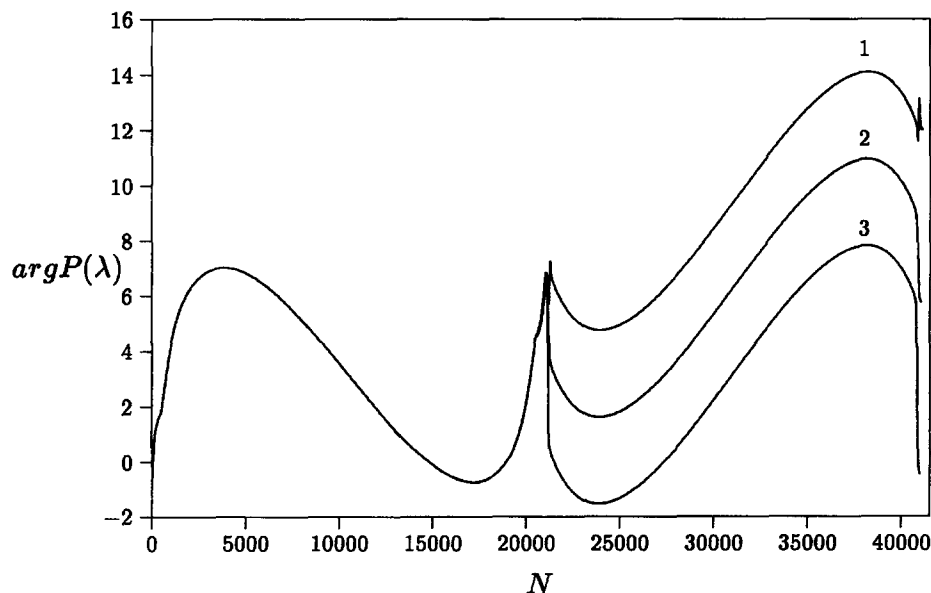


Fig. 2. The variation of the  $\arg P(\lambda)$  along a contour for a Hopf bifurcation point of the system (10) for  $h = 5 \cdot 10^{-3}$  (curve 1),  $h = 10^{-3}$  (curve 2),  $h = 10^{-4}$  (curve 3).  $N$  denotes the numbering of the points along the contour for  $h = 10^{-4}$ .

(curve 1),  $h = 10^{-3}$  (curve 2) and  $h = 10^{-4}$  (curve 3). The value of  $\arg P(\lambda)$  changes quickly ( $d(\arg P(\lambda))/d\lambda > 10^4$ ) in the neighbourhood of points  $\lambda = 10^{-3} \pm 0.9832i$  ( $N = 21\,169$  and  $N = 40\,833$ , respectively). Using  $h = 5 \cdot 10^{-3}$  and  $h = 10^{-3}$  does not lead to a sufficient number of points on these parts of the contour to obtain full information about the variation of  $\arg P(\lambda)$ . As  $\lambda$  moves once along the rectangle, we twice omit the change of  $\arg P(\lambda)$  by  $2\pi$  (in the neighbourhood of  $\lambda = 10^{-3} \pm 0.9832i$ ) for  $h = 5 \cdot 10^{-3}$ . For  $h = 10^{-3}$  we omit the change of  $\arg P(\lambda)$  by  $\pi$  in the same parts of the contour. As a result, the computed variation of  $\arg P(\lambda)$  is  $4\pi$  and  $2\pi$  in these cases while it is equal to zero for  $h = 10^{-4}$ . This implies that we obtain a wrong value for the number ( $N_z$ ) of the roots of  $P(\lambda)$  within the considered contour for relatively large values of  $h$  ( $N_z = 2$  for  $h = 5 \cdot 10^{-3}$  and  $N_z = 1$  for  $h = 10^{-3}$ ) and the correct result ( $N_z = 0$ ) for  $h = 10^{-4}$ .

This example shows that for the stability analysis of Hopf bifurcation points, the step size  $h$  along the part of a contour  $C$  close to the imaginary axis ( $C_1$ ) must be small enough to ensure that the variation of  $\arg P(\lambda)$  between two points of the discretization of  $C_1$  is less than  $\pi$ . Numerous experiments have shown that value  $h = \alpha_{\min}/10$  is suitable to obtain the correct result. An increase of  $\alpha_{\min}$  (and, hence, of  $h$ ) significantly decreases the computational cost of the method. However, in this case the variation in the number of zeros of  $P(\lambda)$  within the contour can only be detected when eigenvalues which have crossed the imaginary axis will be within this contour. Nevertheless, numerical experiments have shown that such rough approximation of points at which a bifurcation of higher singularity occurs is suitable to calculate these points with sufficient accuracy within a continuation procedure. These points can then be used as initial points to compute new branches via continuation.

### 3. Continuation of a branch of Hopf points

In this section we introduce a determining system for Hopf points, describe the choice of the initial point to start tracing of a branch of Hopf points and show how bifurcations of higher singularity can be detected during the continuation of a branch of Hopf points.

To compute Hopf bifurcation points of (1) we follow the method presented in [12] which allows to construct a nonsingular system that “algebraically” determines these points for a system of ODEs as well as for DDEs.

Assume that the system (1) contains two active parameters  $\mu_1$  and  $\mu_2$  (all other parameters are fixed at some particular value). Hopf bifurcation, i.e., the onset of periodic solutions, occurs at a steady-state solution  $(x^H, \mu_1^H, \mu_2^H)$  of (1) for which the characteristic matrix  $\Delta(x^H, \mu_1^H, \mu_2^H, \lambda)$  has a pair of single purely imaginary eigenvalues

$$\lambda = \pm i\omega^H \quad (\omega^H > 0).$$

Hence the following equality is fulfilled:

$$(\Delta_{\text{Re}}(x^H, \mu_1^H, \mu_2^H, i\omega^H) + i\Delta_{\text{Im}}(x^H, \mu_1^H, \mu_2^H, i\omega^H))(\Phi_{\text{Re}}^H + i\Phi_{\text{Im}}^H) = 0, \quad (5)$$

where  $\Delta = \Delta_{\text{Re}} + i\Delta_{\text{Im}}$  and  $\Phi^H = \Phi_{\text{Re}}^H + i\Phi_{\text{Im}}^H$  is the eigenvector corresponding to  $\lambda = i\omega^H$ .

A determining system for Hopf bifurcation is

$$\begin{aligned}
 F(x, x, \dots, x, \mu_1, \mu_2) &= 0, \\
 \Delta_{\text{Re}}(x, \mu_1, \mu_2, i\omega) \Phi_{\text{Re}} - \Delta_{\text{Im}}(x, \mu_1, \mu_2, i\omega) \Phi_{\text{Im}} &= 0, \\
 \Delta_{\text{Re}}(x, \mu_1, \mu_2, i\omega) \Phi_{\text{Im}} + \Delta_{\text{Im}}(x, \mu_1, \mu_2, i\omega) \Phi_{\text{Re}} &= 0, \\
 c^T \Phi_{\text{Re}} &= 0, \\
 c^T \Phi_{\text{Im}} &= 1,
 \end{aligned} \tag{6}$$

with  $c \in \mathbb{R}^n$  an arbitrary vector. A Hopf bifurcation point corresponds to a solution  $(x^H, \mu_1^H, \mu_2^H, \omega^H, \Phi_{\text{Re}}^H, \Phi_{\text{Im}}^H)$  of the system (6). The two last equations of (6) are needed to uniquely determine the eigenvector  $\Phi$ . The choice of  $c$  is not crucial, but  $c$  should not be orthogonal to span  $\{\Phi_{\text{Re}}^H, \Phi_{\text{Im}}^H\}$ . Following [12], we may state that the solution  $(x^H, \mu_1^H, \mu_2^H, \omega^H, \Phi_{\text{Re}}^H, \Phi_{\text{Im}}^H)$  is isolated at a Hopf bifurcation point and at a fold point, i.e., a steady-state solution of the system (1) for which  $F_x(x, x, \dots, x, \mu_1, \mu_2)$  has zero eigenvalue and  $F_\lambda \notin R(F_x)$ . At a fold point, the system (6) has a solution with  $\omega = 0$  and  $\Phi_{\text{Re}} = 0$ .

The choice of the initial point to start tracing of a branch of Hopf points is a rather complicated problem for which no general solution exists, even for the ODEs case. For a system of DDEs, a guess  $\tilde{y}^0$  (we will use the notation  $y = (x, \mu_1, \mu_2, \omega, \Phi)$  for simplicity) for the initial point  $y^0$  on a Hopf bifurcation curve can be found in two ways. First, by solving the system (1) numerically, we can find an approximate steady-state solution  $\tilde{x}^0$  for a parameter value  $\tilde{\mu}_1^0$  ( $\mu_2 = \tilde{\mu}_2^0$  is fixed) such that for  $\tilde{\mu}_1^0 + \varepsilon$  ( $\varepsilon$  is small) the system (1) has a periodic solution. Second, via the continuation of a branch of steady-state solutions  $x$  of (1) in the space  $(x, \mu_1)$  ( $\mu_2 = \tilde{\mu}_2^0$  is fixed), analysing the stability of each computed point along this branch (as it was shown in Section 2), we can locate with sufficient accuracy a point  $(\tilde{x}^0, \tilde{\mu}_1^0, \tilde{\mu}_2^0)$  at which the characteristic matrix has a pair of purely imaginary eigenvalues. Then, using the standard Newton iteration procedure, we compute the eigenvalue  $\lambda^0 = i\tilde{\omega}^0$  as a root of the polynomial (3) at the obtained point  $(\tilde{x}^0, \tilde{\mu}_1^0, \tilde{\mu}_2^0)$ . The eigenvector  $\tilde{\Phi}^0$  corresponding to the eigenvalue  $\lambda^0 = i\tilde{\omega}^0$  is calculated by solving the linear algebraic system (5) with two normalization conditions (the two last equations in the system (6)). Using the obtained point  $\tilde{y}^0$  we compute the initial point  $y^0 = (x^0, \mu_1^0, \mu_2^0, \omega^0, \Phi^0)$  within the continuation procedure of the LOCBIF package [18]. Numerical experiments presented in the next section show that such procedures are quite efficient, even for a large system of equations.

The continuation scheme of the LOCBIF software package involves, for each point  $y^{(k)}$  ( $k > 0$ ) computed along a curve of Hopf points, the traditional main steps: guessing the next point on the curve (predictor), computing the next point (corrector) and testing the computed point. We will not discuss the continuation procedure in detail (see, e.g., [17, 18]).

If the current point  $y^{(k)}$  is accepted as the next regular point on the curve, we can search for special points on the curve located between points  $y^{(k-1)}$  and  $y^{(k)}$ , assuming that every special point may be detected with the help of an appropriate test function defined along the curve. It can be computed using the same technique as for Hopf points. The continuation code for a system of DDEs locates three types of special points on a Hopf bifurcation curve: (a) turning points, (b) self-crossing points and (c) fold points.



Turning points are local extremum points with respect to an active system parameter along the curve. They only characterize geometric properties of the curve to be traced. At a turning point the corresponding component of the tangent vector to the curve becomes zero and it is used as the test function to detect this point.

Self-crossing points are points for which the characteristic matrix has two distinct pairs of purely imaginary eigenvalues

$$\lambda_{1,2} = \pm i\omega_1, \quad \lambda_{3,4} = \pm i\omega_2 \quad (\omega_1 \neq \omega_2),$$

where  $\lambda_{1,2} = \pm i\omega_1$  are eigenvalues computed along the curve. The case  $\omega_1 = \omega_2$  is a degenerate case which we do not consider further. Self-crossing points also characterize the geometry of the curve itself, but these points are bifurcation points of (1). Such points are detected during the stability analysis of each point at the curve: a change in the number of eigenvalues with positive real part at point  $y^{(k)}$  indicates that there is a self-crossing point on the curve between points  $y^{(k-1)}$  and  $y^{(k)}$ . Note that at a self-crossing point the determining system (6) is nonsingular, which allows to use such a point as the initial point to start tracing another branch of Hopf points. The value  $\omega_2$  can be computed as a root of the polynomial (3) using a Newton iteration procedure.

Since at a fold point the Jacobian matrix  $F_x(x, x, \dots, x, \mu_1, \mu_2)$  is singular, the function  $\det(F_x(x, x, \dots, x, \mu_1, \mu_2))$  can be used as the test function to detect fold points in the system (1). Two cases are possible when a fold point is located during continuation of a branch of Hopf points:

$$\lambda_{1,2} = \pm i\omega_1, \quad \lambda_3 = 0, \tag{7a}$$

$$\lambda_1 = 0, \quad \lambda_2 = 0. \tag{7b}$$

Case (a) means that there is the intersection of the Hopf bifurcation curve with a fold bifurcation curve, and case (b) is referred to as a Bogdanov–Takens singularity. In the former case, the determining system (6) is nonsingular, in the latter case system (6) is singular. It is not possible to switch directly to a curve of Bogdanov–Takens points, but, as numerical experiments have shown, a small perturbation of such points is sufficient to start tracing this curve.

#### 4. Results of numerical experiments

In this section we present the results of the numerical study of Hopf bifurcations in a “discrete” version of the Olmstead model [20],

$$\begin{aligned} \frac{du}{dt} = & \frac{1-\delta}{v} (w_0 u_{xx}(x, t) + w_1 u_{xx}(x, t - \tau_1) + w_2 u_{xx}(x, t - \tau_2)) \\ & + \delta u_{xx}(x, t) + Ru(x, t) - u^3(x, t), \end{aligned} \tag{8}$$

which is obtained by the Simpson’s rule approximation of the Olmstead model, describing the flow of a viscoelastic fluid (i.e., a fluid with a “fading memory”),

$$\frac{du}{dt} = \int_{-\infty}^t \frac{1-\delta}{v} e^{-(t-s)/v} u_{xx}(x, s) ds + \delta u_{xx}(x, t) + Ru(x, t) - u^3(x, t), \tag{9}$$

on  $x \in I = (0, \pi)$  with the boundary conditions  $u(0, t) = u(\pi, t) = 0$ . Here  $u(x, t)$  is the velocity of the fluid,  $\nu, \delta, R$  are parameters of the problem,  $\tau_1, \tau_2$  are time delays,  $w_0, w_1, w_2$  are weight coefficients of the quadrature formula, slightly adapted such that  $w_0 + w_1 + w_2 = \nu$  and the systems (8) and (9) have the same nontrivial steady-state solution for fixed values of parameters.

The classical method to study the integro-differential equation (9) is the conversion of (9) into a pair of coupled differential equations without the integral (which represents a continuous delay). Our aim here is not the investigation of (9) as a model of real physical phenomena. Eq. (8) is only a suitable mathematical equation to test the numerical techniques described above and to compare results with known results for model (9) presented, e.g., in [20].

We use the following finite-difference discretization in space to approximate (8) by the system of DDEs:

$$\frac{du_i}{dt} = \frac{1-\delta}{\nu} \sum_{j=0}^2 w_j f(u_{i-1}(s_j), u_i(s_j), u_{i+1}(s_j)) + \delta f(u_{i-1}(t), u_i(t), u_{i+1}(t)) + Ru_i(t) - u_i^3(t), \quad (10)$$

where  $i = 1, \dots, n$ ,  $s_j = t - \tau_j$ ,  $\tau_0 = 0$ ,  $f(v_1, v_2, v_3) = (v_1 - 2v_2 + v_3)/h^2$ ,  $u_0(t) = u_{n+1}(t) = 0$ ,  $h = \pi/(n+1)$ ,  $n = 8$ .

Firstly, consider the case of the trivial steady-state solution of (10) for which some analytic results can be obtained. In this case the characteristic matrix (2) of system (10) is an  $n \times n$  three-diagonal symmetric matrix with equal elements along each diagonal. Its eigenvalues can be computed from the equation [23]

$$\lambda_s = a + 2b \cos \frac{s\pi}{n+1}, \quad s = 1, \dots, n, \quad (11)$$

where

$$a = -2b + R, \quad b = \frac{1-\delta}{\nu h^2} (w_0 + w_1 e^{-\lambda_s \tau_1} + w_2 e^{-\lambda_s \tau_2}) + \frac{\delta}{h^2}.$$

Note that for each value of  $s$  ( $s = 1, \dots, n$ ) one or more eigenvalues  $\lambda_s$  can be computed from (11). This is due to the discrete delays which lead to periodic right-hand sides of (11) and hence to a multitude of solutions. Therefore, we will further use the notation  $\lambda_{s,i}$  with  $i = 1, \dots, ns(s)$ . Let  $\lambda = \alpha + i\omega$ . Two distinct critical cases are possible.

(1) If  $\lambda_{s,i} = 0$ , then there is a sequence

$$R_s^P = \frac{2(n+1)^2}{\pi^2} \left( 1 - \cos \frac{s\pi}{n+1} \right), \quad s = 1, \dots, n,$$

such that for each  $R = R_s^P$  there is a pitchfork bifurcation and two nontrivial steady-state solutions emerge from the trivial solution.

(2) If  $\lambda_{s,i} = i\omega_{s,i}$ , then two equations can be derived which determine values of  $R$  and  $\omega$  at which a Hopf bifurcation occurs and a periodic solution arises from the trivial solution:

$$\begin{aligned}\omega_{s,i}^H &= \frac{2(1-\delta)(n+1)^2}{v\pi^2} (w_1 \sin \omega_{s,i}^H \tau_1 + w_2 \sin \omega_{s,i}^H \tau_2) \left(1 - \cos \frac{s\pi}{n+1}\right), \\ R_{s,i}^H &= \frac{2(1-\delta)(n+1)^2}{v\pi^2} (w_0 + w_1 \cos \omega_{s,i}^H \tau_1 + w_2 \cos \omega_{s,i}^H \tau_2) \left(1 - \cos \frac{s\pi}{n+1}\right), \\ s &= 1, \dots, n, \quad i = 1, \dots, ns(s).\end{aligned}\tag{12}$$

The projections on the  $(R, \delta)$ -plane of all Hopf points and pitchfork bifurcation points on the trivial steady-state solution for  $s = 1, \dots, 4$  are presented in Fig. 3 ( $v = 2, \tau_1 = 3, \tau_2 = 6$ ). Curve 1 is the first Hopf curve. Hopf curves which touch pitchfork curves at points  $B_i$  ( $i = 1, \dots, 4$ ) correspond to the bifurcation values  $R_{s,1}^H$  ( $s = 1, \dots, 4$ ) and they are almost the same curves as for the system (9). The other Hopf curves correspond to values  $R_{3,2}^H, R_{4,2}^H, R_{4,3}^H$  and they do not exist for (9).

The values  $\omega^0$  and  $R^0$  for the initial point on the first Hopf curve were found from (12) for  $s = 1, i = 1, v = 2, \tau_1 = 3, \tau_2 = 6, \delta = \delta^0$ . Then, an eigenvector  $\Phi^0$  corresponding to  $\lambda = i\omega^0$  was computed by solving (5) with normalization conditions  $c^T \Phi_{\text{Re}}^0 = 0, c^T \Phi_{\text{Im}}^0 = 1$ .

All points  $B_i$  on this figure are Bogdanov–Takens bifurcation points, while points on the intersection of Hopf and pitchfork curves are points of type (7a). We also found self-crossing points

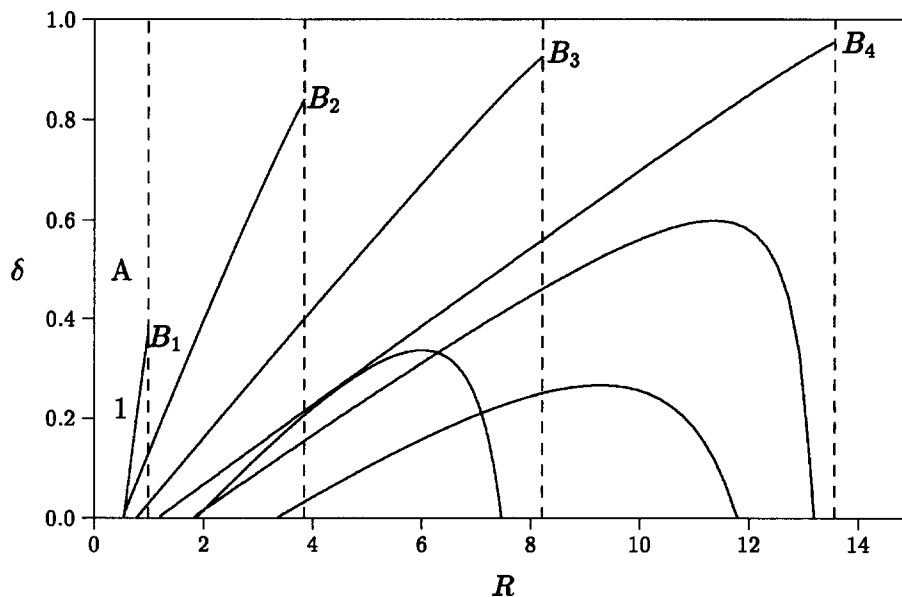


Fig. 3. Curves of Hopf points (full lines) and curves of pitchfork bifurcation points (dashed lines) of the trivial steady-state solution of the system (10). Curve 1 is the first Hopf curve. Region A is the region of existence of the stable trivial solution. Points  $B_i$  ( $i = 1, 2, 3, 4$ ) are Bogdanov–Takens bifurcation points.

at which two Hopf curves intersect each other (these points are characterized by two distinct pairs of purely imaginary eigenvalues). Note that the initial points of all Hopf bifurcation curves can be found with the help of (12) as well as by using self-crossing points which also exist in the region  $\delta < 0$ . The trivial steady-state solution is stable in region A, bounded by the first Hopf and pitchfork bifurcation curves. All Hopf bifurcations destabilize this solution.

To compute the number of eigenvalues with positive real part for each point on the Hopf curves, we applied the argument principle, as described in Section 2, to the rectangular contour with  $\alpha_{\min} = 10^{-2}$ ,  $\alpha_{\max} = 5$ ,  $\omega_{\max} = 5$ . Numerical experiments have shown that this contour is sufficient to detect all eigenvalues lying to the right of the imaginary axis. For points  $\lambda_c$  on the contour, the characteristic polynomial  $P(\lambda)$  has been numerically evaluated as the value of  $\det \Delta(x^H, \mu^H, \lambda_c)$ , where  $(x^H, \mu^H)$  is a Hopf point on the curve.

Fig. 4 shows the regions in the  $(R, \delta)$ -plane where stable solutions of the system (10) exist: the trivial steady-state solution (A), two nontrivial steady-state solutions (B) and periodic solutions (C). Two unstable nontrivial solutions arising from a pitchfork bifurcation become stable after one, two or three Hopf bifurcations (this depends on the value of  $\delta$  if the value of  $R$  is fixed).

The first Hopf bifurcation curve for nontrivial steady-state solutions consists of three parts of different branches of Hopf points. A guess for the initial point on this curve was obtained by the procedure described in Section 3. Starting from this point, we computed one of the three branches presented in this figure. Two other branches of Hopf bifurcation points on nontrivial steady-state solutions were traced from self-crossing points, detected during the computation of previous branches. For each point on these curves the number of eigenvalues with positive real part was

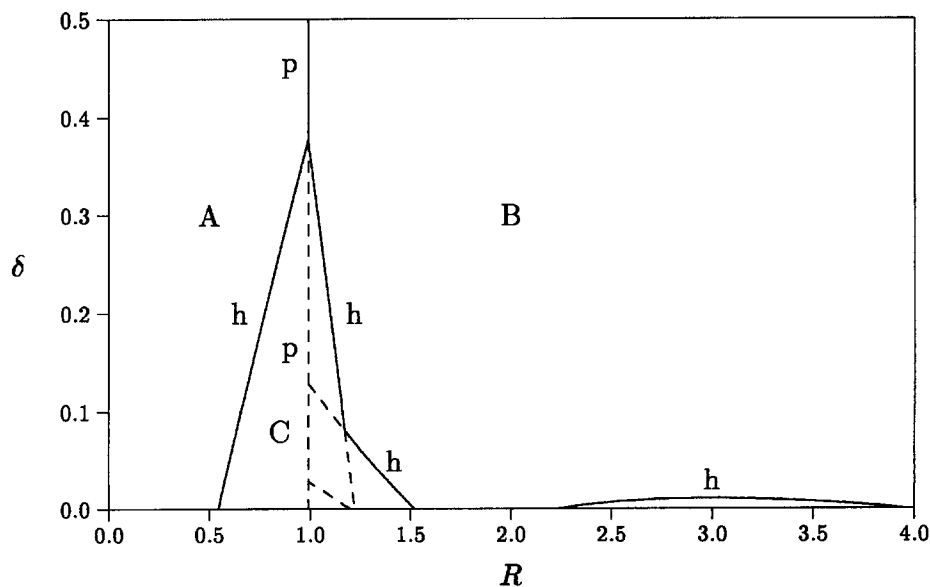


Fig. 4. The regions of existence of stable solutions of the system (10). A: the trivial steady-state solution; B: two nontrivial steady-state solutions; C: periodic solutions. These regions are bounded by parts of Hopf curves (denoted with (h)) and pitchfork curves (denoted with (p)).

computed in the same way as for the trivial solution. To locate self-crossing points accurately, we used  $\alpha_{\min} = 10^{-3}$  and we decreased the step size  $h$  to  $h = 10^{-4}$  along the part of the considered contour close to the imaginary axis.

## 5. Conclusion

We have presented a numerical technique for the stability analysis and the computation of branches of Hopf bifurcation points in nonlinear systems of delay differential equations (DDEs) with several constant delays. This technique has been implemented within the LOCBIF software package [18]. The stability analysis of a steady-state solution of a system of DDEs is done by the numerical implementation of the argument principle which allows to compute the number of eigenvalues with positive real part of the characteristic matrix. The application of this method to the stability analysis of Hopf bifurcation points, as a special case, is also quite efficient. To use the method, we do not need to know the explicit expression of the characteristic equation. This is especially important when the dimension of a system of DDEs or the number of delays is large.

The use of a determining system for Hopf bifurcation points allows to trace branches of Hopf points via continuation. The continuation procedure also detects bifurcations of higher singularity during tracing of a branch of Hopf points: self-crossing points (for which the characteristic matrix has two distinct pairs of purely imaginary eigenvalues) and fold points. The nonsingularity of the determining system at these points allows to use such points as the initial points to start tracing of a new branch of Hopf points or a fold curve.

As mentioned above, we consider the computation of branches of Hopf bifurcation points as the first step in the numerical bifurcation analysis of DDEs. The bifurcation analysis of periodic solutions can be the next one.

## Acknowledgements

This text presents research results of the Belgian programme on Interuniversity Poles of Attraction (IUAP 17), initiated by the Belgian State – Prime Minister’s Service – Federal Office for Science, Technical and Cultural Affairs (OSTC). The scientific responsibility is assumed by its authors. T. Luzyanina has been funded by a fellowship of OSTC.

## References

- [1] C.T.H. Baker, C.A.H. Paul and D.R. Willé, A bibliography on the numerical solution of delay differential equations, Techn. Report 269, Univ. of Manchester, Manchester Centre for Computational Mathematics, 1995.
- [2] H.T. Banks and F. Kappel, Spline approximations for functional differential equations, *J. Differential Equations* **34** (1979) 469–522.
- [3] R. Bellman and K.L. Cooke, *Differential-Difference Equations*, Mathematics in Science and Engineering, Vol. 6 (Academic Press, New York, 1963).
- [4] A.M. Castelfranco and H.W. Stech, Periodic solutions in a model of recurrent neural feedback, *SIAM J. Appl. Math.* **47** (1987) 573–588.

- [5] S.-N. Chow and J. Mallet-Paret, Integral averaging and bifurcation, *J. Differential Equations* **26** (1977) 112–159.
- [6] J.R. Claeysen, The integral-averaging bifurcation method and the general one-delay equation, *J. Math. Anal. Appl.* **78** (1980) 429–439.
- [7] J.C. Fernandes de Oliveira and J.K. Hale, Dynamic behavior from bifurcation equations, *Tôhoku Math. J.* **32** (1980) 577–592.
- [8] R.D. Driver, *Ordinary and Delay Differential Equations*, Applied Mathematical Science, Vol. 20 (Springer, Berlin, 1977).
- [9] L.E. El'sgol'ts and S.B. Norkin, *Introduction to the Theory and Application of Differential Equations with Deviating Arguments*, Mathematics in Science and Engineering, Vol. 105 (Academic Press, New York, 1973).
- [10] J.D. Farmer, Chaotic attractors of an infinite-dimensional dynamical system, *Physica D* **4** (1982) 366–393.
- [11] J.M. Franke and H.W. Stech, Extensions of an algorithm for the analysis of nongeneric Hopf bifurcations, with applications to delay-difference equations, in: S. Busenberg and M. Martelli, Eds., *Delay Differential Equations and Dynamical Systems*, Lecture Notes in Mathematics, Vol. 1475 (Springer, Berlin, 1990) 161–175.
- [12] A. Griewank and G. Reddien, The calculation of Hopf points by a direct method, *IMA J. Numer. Anal.* **3** (1983) 295–303.
- [13] J.K. Hale, *Theory of Functional Differential Equations*, Applied Mathematical Science, Vol. 3 (Springer, Berlin, 1977).
- [14] J.K. Hale, Nonlinear oscillations in equations with delays, in: F.C. Hoppensteadt, Ed., *Nonlinear Oscillations in Biology*, Lectures in Applied Mathematics, Vol. 17 (Amer. Mathematical Soc., Providence, RI, 1979) 157–185.
- [15] J.K. Hale, Dynamics and delays, in: S. Busenberg and M. Martelli, Eds., *Delay Differential Equations and Dynamical Systems*, Lecture Notes in Mathematics, Vol. 1475 (Springer, Berlin, 1990) 16–30.
- [16] B.D. Hassard, N.D. Kazarinoff and Y.-H. Wan, *Theory and Applications of Hopf Bifurcation*, London Mathematical Society Lecture Note Series, Vol. 41 (Cambridge Univ. Press, Cambridge, 1981).
- [17] A.I. Khibnik, Yu.A. Kuznetsov, V.V. Levitin and E.N. Nikolaev, LOCBIF: Interactive Local Bifurcation Analyzer, version 2.2, Institute of Mathematical Problems in Biology, Russian Academy of Sciences, Pushchino, 1992.
- [18] A.I. Khibnik, Yu.A. Kuznetsov, V.V. Levitin and E.N. Nikolaev, Continuation techniques and interactive software for bifurcation analysis of ODEs and iterated maps, *Physica D* **62** (1993) 360–371.
- [19] V.B. Kolmanovskii and A. Myshkis, *Applied Theory of Functional Differential Equations*, Mathematics and its Applications, Vol. 85 (Kluwer Academic Publishers, Dordrecht, 1992).
- [20] W.E. Olmstead, S.H. Davis, S. Rosenblat and W.L. Kath, Bifurcation with memory, *SIAM J. Appl. Math.* **46** (1986) 171–188.
- [21] W.C. Rheinboldt, D. Roose and R. Seydel, Aspects of continuation software, in: D. Roose, B. De Dier and A. Spence, Eds., *Continuation and Bifurcations: Numerical Techniques and Applications*, NATO ASI Series, Vol. 313 (Kluwer Academic Publishers, Dordrecht, 1989) 261–268.
- [22] H.W. Stech, Nongeneric Hopf bifurcation in functional differential equations, *SIAM J. Math. Anal.* **16** (1985) 1134–1151.
- [23] J.H. Wilkinson, *The Algebraic Eigenvalue Problem* (Clarendon Press, Oxford, 1978).
- [24] X. Ying and I.N. Katz, A reliable argument principle algorithm to find the number of zeros of an analytic function in a bounded domain, *Numer. Math.* **53** (1988) 143–163.
- [25] X. Ying and I.N. Katz, A simple reliable solver for all the roots of a nonlinear function in a given domain, *Computing* **41** (1989) 317–333.